Yearly Progress Report

DE-FG07-02ID14326

Insulation for a Thermionic Microbattery

Professor James P. Blanchard

Department of Engineering Physics

University of Wisconsin

1500 Engineering Dr.

Madison, WI 53706

(608) 263-0391

(608) 263-7451 (FAX)

blanchard@engr.wisc.edu

http://www.engr.wisc.edu/ep/faculty/blanchard_james.html

Subcontractor: Sandia National Laboratory

Summary of Proposed Work

Microelectromechanical Systems (MEMS) have not gained wide use because they lack the on-device power required by many important applications. To supply this needed power, one can consider power from fossil fuels, but nuclear sources provide an intriguing option in terms of power density and lifetime. In order to make use of alpha particles, one is forced to use thermal approaches because diodes are damaged by the high energy of the alphas. One difficulty, though, is that the surface to volume ratio increases as we move to smaller scales and heat losses thus become significant at MEMS scales. Hence, efficient microscale insulation is needed to permit high overall efficiencies. This research explores concepts for one variety of microscale insulation created using MEMS fabrication techniques.

The preliminary design for the micro-insulation is shown schematically in the figure below. The focus of the design is a GaAs wafer that is approximately 0.625 mm thick and 70 mm in diameter. A 100 nm epitaxial layer of AlAs followed by a 2000 nm layer of GaAs is then deposited. The AlAs layer serves as an etch stop. A membrane of GaAs is created by jet etching from the back of the wafer using a gold mask. The jet etchant stops at the AlAs layer, which is then removed in dilute HF. The GaAs membrane is coated with a high-reflection (HR) coating. Underneath this layer is a high reflectivity coating. Suspended above the GaAs wafer by the GaAs spikes is a silicon wafer with a highly reflective coating. These spikes minimize the contact area and thus minimize conduction losses.

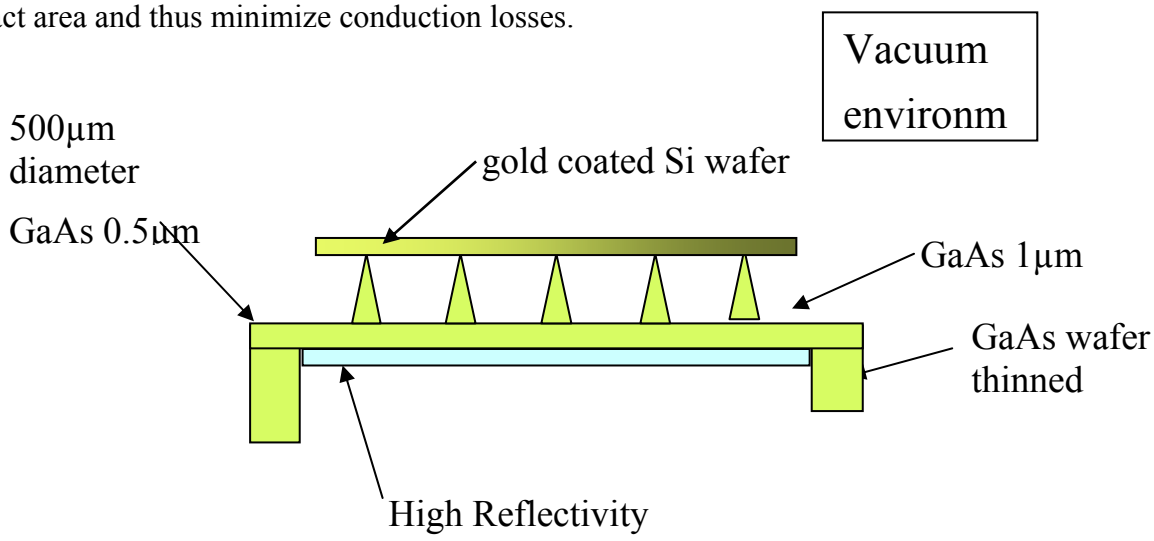

Figure 1: Preliminary design for microinsulation

The following tasks were proposed for Phase I of this two-year project:

1. Fabricate insulator sample using preliminary design
2. Develop thermal and structural models for insulator
3. Measure thermal conductance of preliminary insulator
4. Use measured results, along with simulations, to optimize insulator design

Fabrication

The fabrication of a test article at Sandia National Laboratories' Compound Semiconductor Research Laboratory (CSRL) is underway. The developmental stages were as follows:

- A decision was made to produce test articles in two stages. The first test article consists of chips with trial productions of spike layers. The second test article will include the spike layer, a thinned membrane, and a reflective coating. An analysis was completed to determine a range of spacings between spikes for testing.
- A quarter-wafer mask was fabricated for the spike-layer test articles. The pattern for the quarter-wafer is shown in Figure 2. The first number in each box refers to the bottom diameter of each spike (1/2 or 1 micron). The second number refers to the spacing between spikes (10 50 or 100 microns. Each spike is 1 micron tall. The 3 mm x 3mm boxes represent the area covered by each set of spikes. The pitch between patterned areas is 5 mm.
- Several trial runs were made to determine the appropriate method for fabricating spikes using a new type of etching equipment. After several trials, an acceptable method was established, and the test articles were fabricated, as shown in the micrographs in Figure 3.
- The MHB spike-layer test articles were passed to the University of Wisconsin for testing.
- Fabrication of the membrane for the next set of test particles began. A GaAs wafer was grown with a wet etch stop layer and 2 microns of GaAs to serve as a membrane.

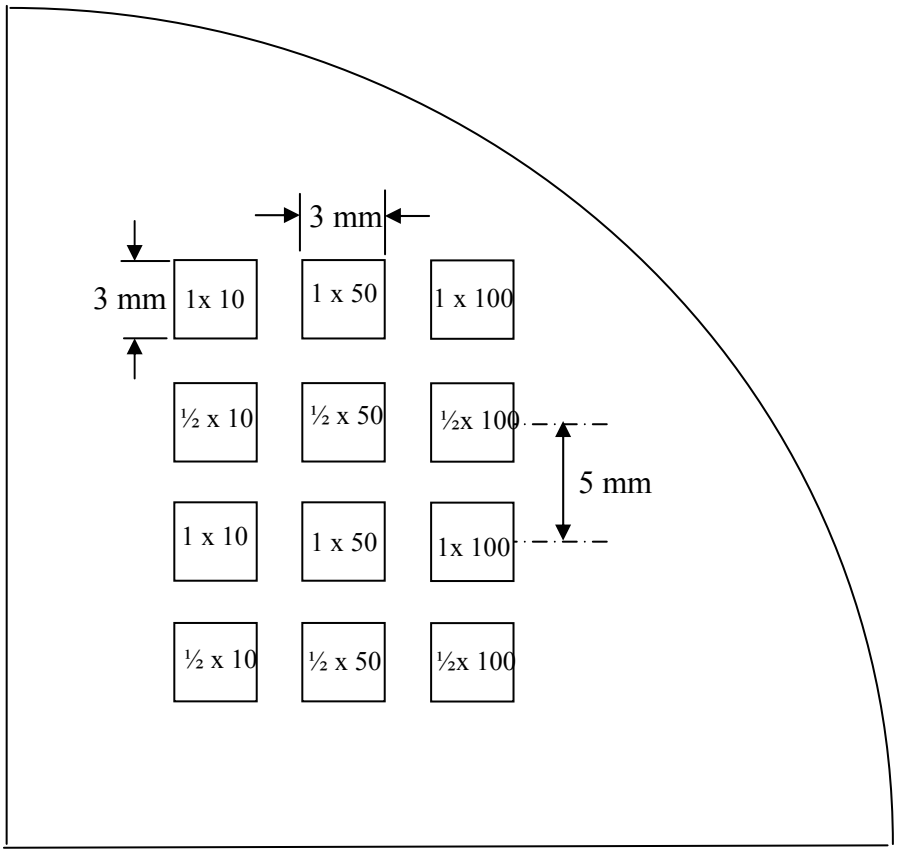

Figure 2 Patterned MHB 1/4 Wafer

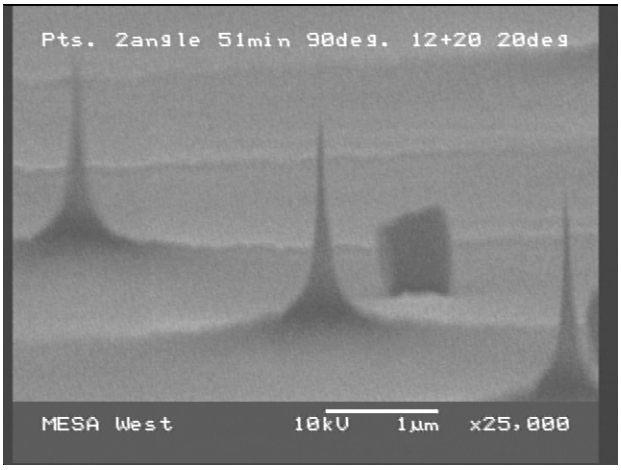

Figure 3 Micro Heat Barrier spike etches.

Modeling

Maximum Displacement in a Circular Plate

One key design parameter is the spacing of the cones supporting one surface of the micro heat barrier (MHB) above the other. These cones must be far enough apart to reduce conduction through them relative to radiation from surface to surface, but they must be close enough to prevent the upper surface from collapsing. We will first address the support issue, modeling the upper surface as a circular plate with the diameter approximately equal to the cone spacing. The edges of this plate are modeled as simply supported in one case, and clamped in a second case. The load is from the weight of the plate and the maximum displacement δ_{max} occurs at the center. We take the displacement limit to be approximately the plate spacing (1 micron).

For a simply supported edge and uniform load[1],

$$\delta_{\max} = \frac{3}{16}(1-\nu)(5+\nu)\frac{wR^4}{Et^3}$$

where ν is Poisson's ratio, w is uniform load per unit area, t is plate thickness, R is plate radius, E is elastic modulus. For fixed edge and uniform load,

$$\delta_{\max} = \frac{3}{16}(1-\nu^2)\frac{wR^4}{Et^3}$$

The displacements are shown in the figure below. As can be seen, the separation can be quite large. Hence, the failure mechanism is more likely collapse of the cones, rather than collapse of the upper plate.

[1] Fred B. Seely, James O. Smith, *Advanced Mechanics of Materials*, second edition, John Wiley & Sons, 1959

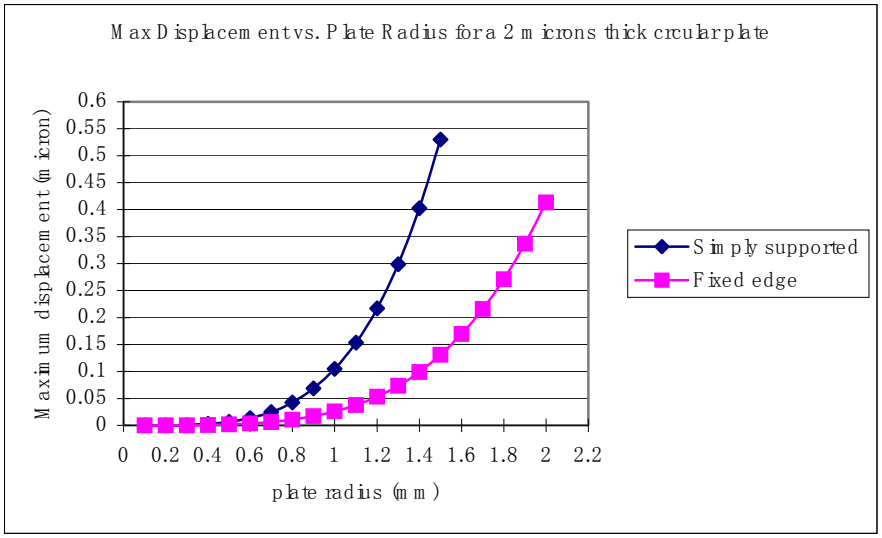

Figure 4: Maximum Displacement for a 2 micron thick circular plate

Thermal Conductivity of Air at Low Pressure

In order to minimize conduction through the MHB, the gas pressure between the layers must be kept to a minimum. The necessary pressure can be chosen by ensuring that conduction through the gas is small compared to the radiation through it. Because the gas pressure will be quite small, macroscopic models for gas conduction are not valid and we must take care to accurately represent the conductivity. From a simple kinetic-theory model[2] the thermal conductivity is

$$k_{gas} = \frac{1}{3}\rho \overline{w} \lambda c_v$$

where ρ is the density, w is the average molecule velocity, λ is the mean free path of the particles in the gas, and c_v is the heat capacity. Similarly, dynamic viscosity is

$$\mu = \frac{1}{3}\rho \overline{w} \lambda$$

so

$$k_{gas} = \mu \cdot c_v$$

[2] E.R.G. Eckert, Robert M. Drake, JR., *Analysis of Heat And Mass Transfer*, MaGraw-Hill, 1972

Eucken used this relationship to account for internal degrees of freedom in the molecule

$$k_{gas}^{\ Eucken} = \mu\left(c_v + \frac{9}{4}\frac{R}{M}\right) = \frac{1}{4}(9\gamma - 5)\mu \cdot c_v$$

To find $\mu = \frac{1}{3}\rho\overline{w}\lambda$ we can use

$$\rho_{vac} = \rho_{std} \cdot \frac{P_{vac}}{P_{std}} = 0.2947 kg/m^3 \cdot \frac{1.33 Pa}{101325 Pa} = 3.87 \times 10^{-6} kg/m^3$$

$$\overline{w} = \sqrt{\frac{8RT}{\pi M}} = 936 m/s$$

where M is molecular weight, R is the universal gas constant, and T is absolute temperature. Also, the mean free path of gaseous molecules is

$$\lambda = \frac{1}{\sqrt{2}\pi d^2 n}\frac{kT}{\sqrt{2}\pi d^2 P}$$

where d is the diameter of gas molecules, n is the number of molecules per unit volume, k is Boltzman constant, T is temperature, P is pressure. For air, d=2*10^{-10} m, T=1200K, P=10^{-2} Torr, $\lambda = 7cm$

$$\mu = 8.45*10^{-5} \text{ kg/ms}$$

$$C_p = 1.18 \text{ J/kgK at 1200 K}$$

$$c_v = \frac{c_p}{\gamma} = \frac{1.18 J/kg \cdot K}{1.4} = 0.84 J/kg \cdot K$$

$$k_{gas} = 1.35*10^{-4} \text{ W/mK}$$

C. L. Tien[3] gives another relation in terms of macroscopic properties for estimating mean free path

$$\lambda = 8.6\left(\frac{\mu}{P_{vac}}\right)\sqrt{\frac{T}{M}}$$

where μ is viscosity in poise, P_{vac} pressure in millimeters mercury (or Torr), λ is in centimeters. This gives about 5 times lower value than the previous result. For air, $d=2*10^{-10}$ m, T=300K, $P=10^{-2}$ Torr, $\lambda = 0.75\ cm$. Note here that since the mean free path is much larger than the characteristic length (four orders larger than the two-plate spacing), the mean free path bounded by the two plates is limited by the spacing dimensions. So under free-molecule conditions, the mean free path defined above must be replaced by D.

$$\mu = \frac{1}{3}\rho \overline{w} D = 3.6 \times 10^{-9}\, kg/m \cdot s$$

C_p=1.18 J/kgK at 1200 K, air

$$c_v = \frac{c_p}{\gamma} = \frac{1.18 J/kg \cdot K}{1.4} = 0.84 J/kg \cdot K$$

Combining these equations, we find

$$k_{gas} = \frac{1}{12}(9\gamma - 5)\frac{\rho_{std,T} P_{vac}}{P_{std}} \sqrt{\frac{8RT}{\pi M}} \frac{C_p}{\gamma} D$$

which gives $k_{gas}=5.75*10^{-9}$ W/mK.

The thermal conductivity of a gas under free-molecule conditions is decreased as pressure is reduced. This is because when rarefaction increases, the numbers of collisions between gaseous molecules are much less than the numbers of impacts of gaseous molecules on the solid surfaces. In other words, the gaseous molecules strike one surface, then another surface without colliding with one another. So the heat exchanged is proportional to the number of molecules striking both surfaces and consequently proportional to the pressure of the rarefied gas between the two plates.

[3] C. L. Tien, G. R. Cunnington, *Cryogenic Insulation Heat Transfer*, Advances in Heat Transfer, Academic Press, Inc. Vol. 9, 1973

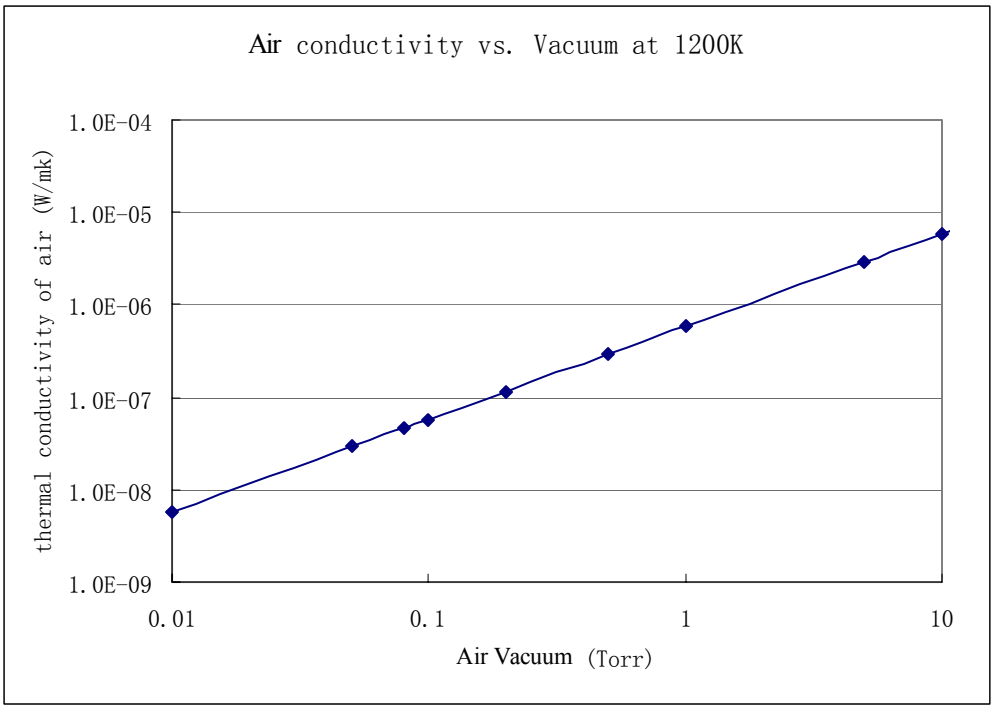

Figure 5: Thermal Conductivity of Air as a Function of Pressure

Using the Fourier law, the heat transfer by gas conduction is given by

$$q'' = \frac{k_{gas}}{D}\Delta T = \frac{1}{12}(9\gamma - 5)\frac{\rho_{std,T} P_{vac}}{P_{std}}\sqrt{\frac{8RT}{\pi M}}\frac{C_p}{\gamma}\Delta T$$

which indicates that the conductive heat flux is independent of the gap spacing D.

The vacuum, here is also important in defining the free-molecule regime (Kn>10). Using this equation will give more conservative results for estimating the required vacuum to satisfy free-molecular conditions. From the graph below, assuming D is 3 microns, the vacuum must be lower than 5 Torr to ensure Kn>10.

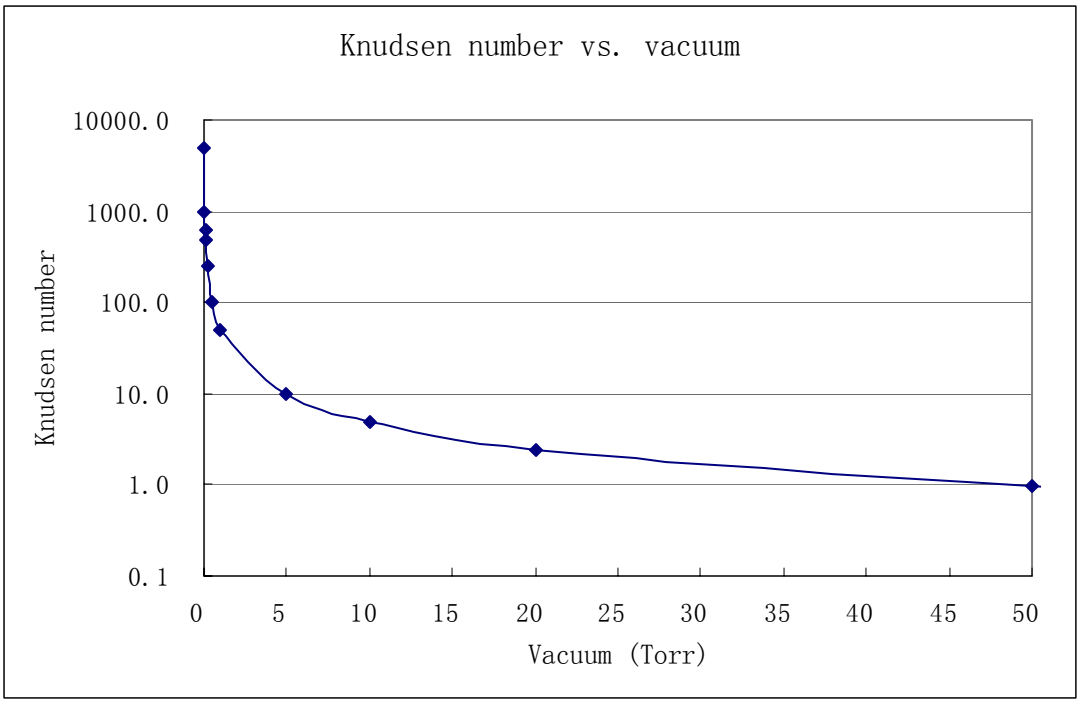

Figure 6: Knudson number for Air

Heat transfer between two plates

This thermal conductivity model can be used to assess the necessary pressure needed for efficient MHB performance. We can simultaneously assess the relative heat transfer through the cones and the gap between the MHB layers. When a constant and uniform heat flux Q is applied to one plate, we can assume one part of heat, Q*f, goes through the cones by conduction and the other part, Q(1-f), goes through vacuum by radiation and conduction of residue air.

Assuming the "cones" have constant cross-section, the thermal resistance of the cones is

$$R_s = \frac{D}{A_s k}$$

where D is the cone length, A_s is the total cross section area of all the cones, and k is the thermal conductivity of GaAs. The thermal resistance of the air is

$$R_g = \frac{D}{A_g k_{gas}}$$

where A_g is the total cross section of gas conduction. The thermal resistance of radiation is

$$R_r = \frac{\frac{1}{\varepsilon_1} + \frac{1}{\varepsilon_2} - 1}{\sigma \cdot A_g \left(T_1^{\,2} + T_2^{\,2}\right)\left(T_1 + T_2\right)}$$

where σ is Stefan-Boltzman constant, ε_1 and ε_2 are emissivities of the inside surfaces of the two plates.

Using these relations, the relative heat transfer rates are given by:

$$Q \cdot f = \frac{T_1 - T_2}{R_s}$$

$$Q \cdot (1 - f) = \frac{T_1 - T_2}{R_g + R_r}$$

The total equivalent thermal conductivity of the MHB is thus

$$k_{eq} = \frac{Q \cdot D}{(T_1 - T_2)(A_s + A_g)}$$

Consider a case where there are a certain number of cones between the two plates, with the distance between any two neighboring cones defined as L. For any single cone, the total heat transferred consists of conduction through its cross section and gas conduction and radiation through the area between the cones. Assuming the cone's diameter is 0.2 microns, the accommodation coefficient is 1, F is 1, ε_1 and ε_2 are 0.9, and the gas pressure between two plates is 5 Torr, where free-conduction condition is just satisfied, the relationship between cone distance and the heat flux fraction and overall thermal conductivity is given below.

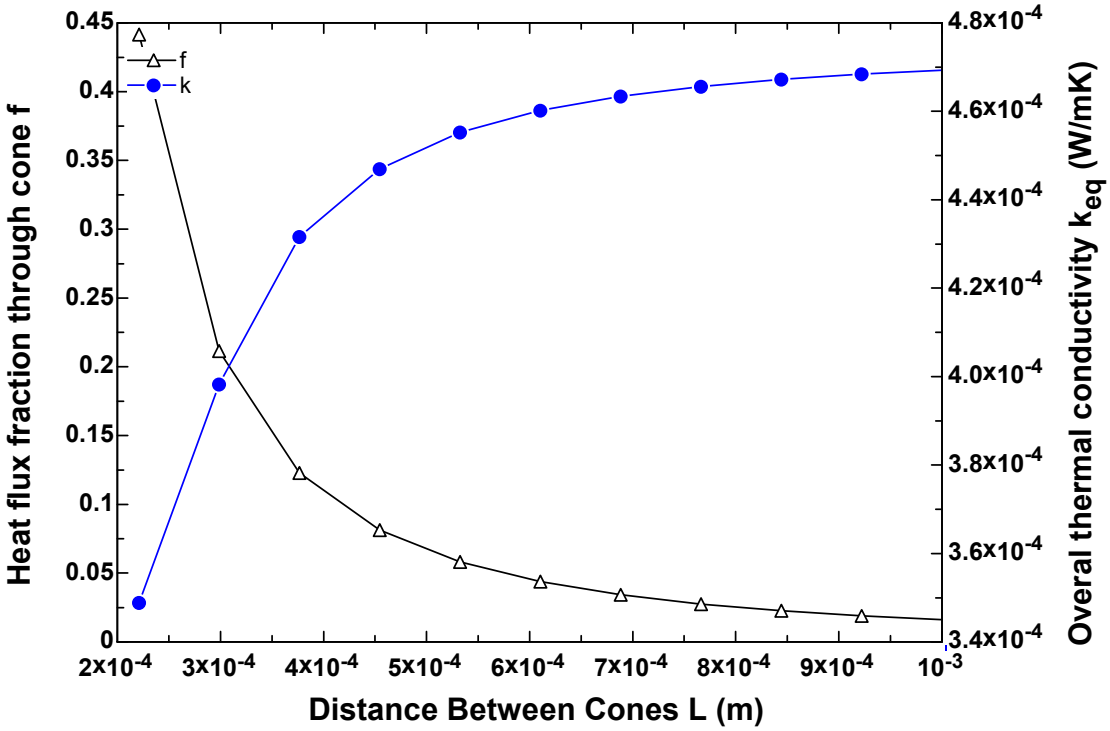

Figure 7: Heat Flux Fraction as a Function of Distance between Cones

As can be seen, cone separations on the order of a few hundred microns are needed to ensure that the heat transfer is dominated by the area between the cones.

The gas conduction is independent of distance between the two plates D, however, the heat conduction through the cones decreases and the overall thermal conductivity increases as the D becomes larger. When $L=5*10^{-4}$m, P=5 Torr, the relationship of D and f, k_{eq} are given below.

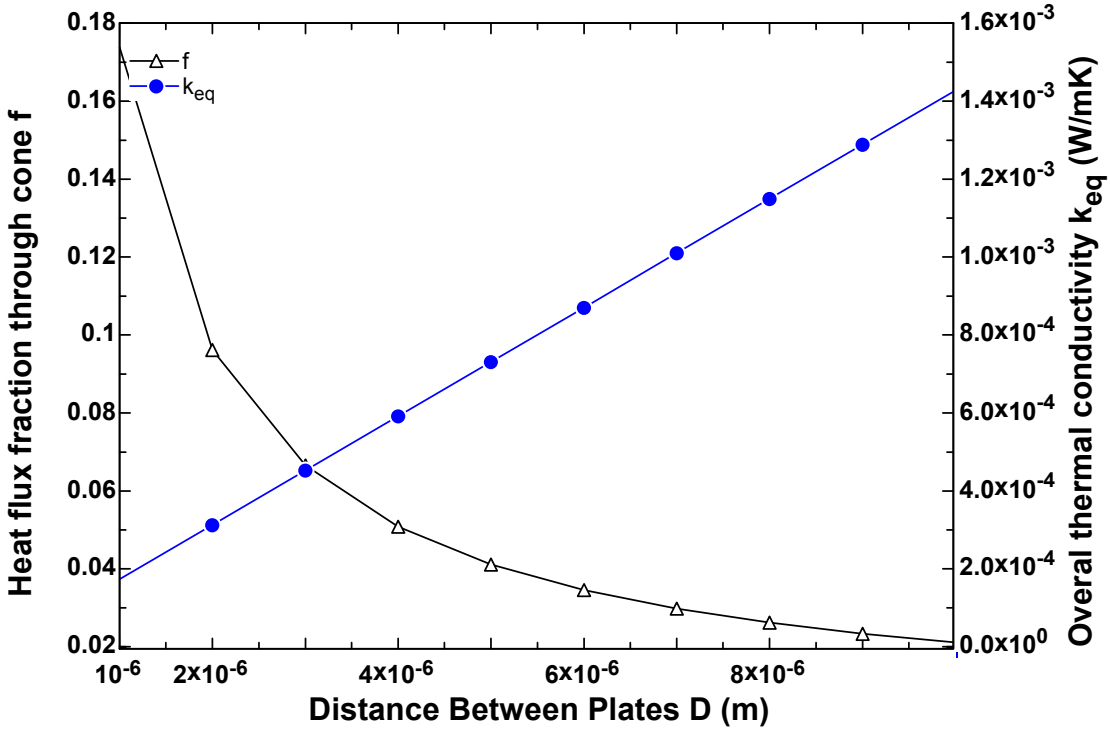

Figure 8: Dependence of Fraction of Heat Transfer Through Cones as a Function of Plate Separation

Monte Carlo Heat Transport

To better model the radiation through the MHB, we have begun development of a Monte Carlo photon transport code to allow us to assess the importance of radiation from the cones. The geometry of the model is shown below

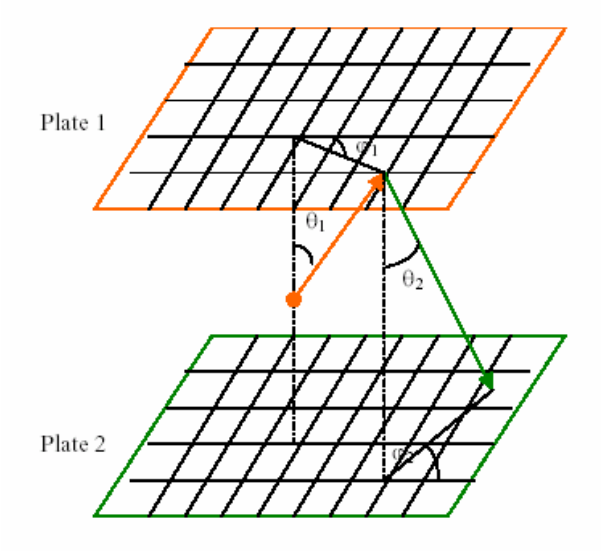

Figure 9: Schematic of Monte Carlo Model

This figure shows a source between two plates and one reflection of a photon off of one plate, towards the second. The surfaces can be modeled as either specular or diffuse. The figure below shows a typical set of intensity contours on the second plate, due to a fan-shaped source reflecting off of both a specular and diffuse first plate. Development of these models is in progress and will help us to better understand heat transfer in the MHB.

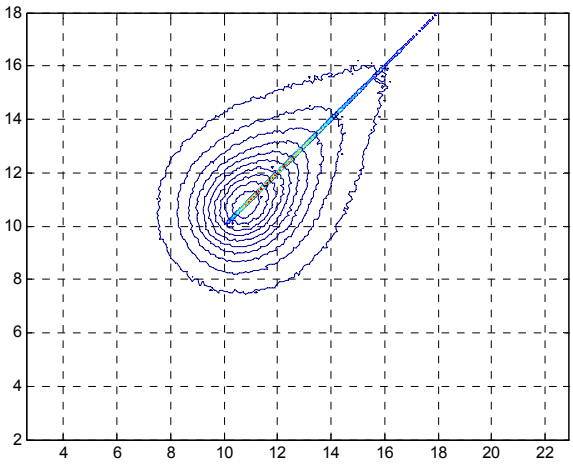

Figure 10: Intensity Contours on Lower Plate Due to Both Specular and Diffuse Reflection

Conductance Measurement

We have not yet completed an evaluation of an MHB design. We have constructed the experimental apparatus, including a vacuum chamber capable of approximately 1 mTorr gas pressures, thermocouples and heat flux sensors for measuring the heat flux through the back of the sample and temperatures on both surfaces. This will allow us to evaluate the transient heat transport and temperature distributions, so that at steady state we can evaluate the conductance (and effective thermal conductivity) of the MHB. This apparatus has been used to measure samples with known conductivities, including high conductivity (copper) and moderate conductivity (ceramic) materials. We are now in a position to begin evaluating the MHB conductance, but have not yet completed a study. This should be completed in approximately two weeks.

Initial Optimization

Because we have not yet evaluated an MHB conductance, we have not yet begun the optimization of the MHB. However, we have created several different MHB devices, with a variety of cone designs, and we will soon be in a position to evaluate the most promising concepts. We also are in the process of developing the membranes that will act as the upper layer in the MHB.

Plans for Second Year

In the coming year, we will complete the measurements of the MHB concepts created to date, update the design based on the measurements, measure the conductance the redesigned MHB, and create a thermionic MEMS battery design based on the MHB results.